A Full Radial Electric Field Calculation for Predicting Pedestal Formation in *H*-mode Tokamak Plasma by using BALDUR code

Y Pianroj*, and S Jumrat
Faculty of Sciences and Industrial Technology, Prince of Songkla University
Suratthani Campus, Surat-Thani, 84000 Thailand
B Chatthong, and T Onjun
School of Manufacturing System and Mechanical Engineering,
Sirindhorn International Institute of Technology, Thammasat University,
Rangsit Campus, Khlong Nueng, Klong Luang, Pathum Thani, 12120 Thailand

Abstract

In this work, a prediction of pedestal formation in *H*-mode tokamak plasma by using the full calculation of the radial electric field (E_r) is performed with three terms of E_r (the pressure gradient, the poloidal velocity, and the toroidal velocity). The E_r is used to compute an important candidate for the edge turbulence stabilization, namely the $\omega_{E\times B}$ flow shear. This full calculation is combined with the model to predict pedestal formation in *H*-mode tokamak plasma based on suppression of anomalous transport that uses the $\omega_{E\times B}$ flow shear and the magnetic shear. All calculations are developed and tested in BALDUR integrated predictive modeling code. The simulations with time evolution of plasma current, ion and electron temperature, and particle and impurity density profiles are compared to the experimental profiles of 10 DIII-D *H*-mode discharges. To validate the agreement between the simulation results and the corresponding experiment results, we carried out a statistical analysis that includes a computation of the root mean square (RMS%) and the offset%. The results show that the predicted plasma profiles yield an overprediction.

Keywords: a radial electric field; tokamak plasma; pedestal; *H*-mode; and BALDUR code.

1. Introduction

Since the high confinement mode (*H*-mode) of tokamak plasmas has been discovered. The *H*-mode generally provides high temperature and excellent energy confinement time. Typically, the energy content in an *H*-mode regime is approximately twice the energy contained in an *L*-mode regime, for a similar plasma with the same input power [1]. Thus, many of burning plasma experiments, not only the Doublet III-Device (DIII-D), Tokamak Fusion Test Reactor (TFTR), and Joint European Torus (JET) were tested in the *H*-mode regime, but also the biggest tokamak, named the International Thermonuclear Experiment Reactor (ITER) [2] is designed to operate in this regime, too.

It is known that the improved performance of *H*-mode results mainly from the formation of an edge transport barrier (ETB) [3], called the pedestal. It is widely

***Correspondence** : yutthapong.p@psu.ac.th

believed that a pedestal reduces a pedestal transport, which can occur due to a stabilization or decorrelation of microturblence in the edge plasma. The stabilization mechanisms, which can suppress turbulent modes, have to take into account the different dynamical behaviors of the various species in the plasma. The first candidate is the magnetic shear stabilization, which is reduced only in the region where the magnetic shear exceeds its threshold. The second candidate is the $\omega_{E\times B}$ flow shear, which is a function of the radial electric field (E_r). It can suppress turbulence by linear stabilization of turbulent modes, and in particular by non-liner decorrellation of turbulence vortices [4-6], thereby reducing transport by acting on both the amplitude of the fluctuations and the phase between them [7].

Theoretically, the calculation of $\omega_{E\times B}$ flow shear requires information about E_r, which can be calculated from three quantities, pressure gradient ($\partial p_i / \partial r$), the poloidal velocity (v_θ), and the toroidal velocity (v_ϕ), as shown in Eq. (9). As a result, it is crucial to develop a model for predicting toroidal velocity in order to predict the ETB formation in *H*-mode. Pianroj Y, et al. [8-9] devised the model for predicting the pedestal based on the suppression of the anomalous transport using magnetic shear and $\omega_{E\times B}$ flow shear. However, the calculation of $\omega_{E\times B}$ flow shear in their work ignored the toroidal velocity. Consequently, the toroidal velocity model in Ref. [10] was developed and implemented via the integrated predictive modeling code BALDUR [11].

In this work, the full calculation of the radial electric field, which consists of three terms, is used to calculate the $\omega_{E\times B}$ flow shear. Then it is substituted in the suppression model, which is composed of two candidates (the magnetic shear and the $\omega_{E\times B}$ flow shear) in order to predict the pedestal formation in the experimental results of 10 DIII-D *H*-mode discharges. This paper is organized as follows. The next section is a brief description of BALDUR code, the anomalous core transport model (Mixed B/gB), the suppression model, and the toroidal velocity model. The third section contains the results and discussion. The conclusion is in the final section.

2. BALDUR code

The BALDUR integrated predictive modeling code [11] is called a 1.5 dimensional code because the transport equations are one-dimensional flux-surface-averaged equations, in which metric elements describe the effects of the two dimensional shapes on the magnetic flux surfaces. Integrated 1.5 dimensional codes are used when the magnetic flux surfaces are closed and when the transport along magnetic field lines is much larger than the transport across the field lines. BALDUR uses theory-based and empirical models to compute self-consistently the source neutral beam injection (NBI) heating, nuclear reaction, radio frequency (RF heating), sink (impurity radiation), energy and particle transport fluxes, magnetohydrodynamic equilibrium, and large scale instabilities (sawtooth oscillations). The BALDUR simulations have been used to predict the time evolution of plasma profiles including electron and ion temperature, hydrogen and impurity densities, safety factor, neutrals and fast ions, for *L*-mode and *H*-mode discharges of conventional tokamaks. BALDUR simulations have been extensively compared with experimental data on plasma and have yielded overall agreements with about a 10% relative RMS deviation [12-13]. In the BALDUR code, fusion heating power is determined by the nuclear reaction rate together with a Fokker-Planck package that computes the slowing of fast alpha particles on each flux surface

in the plasma. The fusion heating component of the BALDUR code also computes the production rate of thermal helium ions and the depletion rates of deuterium and tritium ions within the plasma core.

2.1 Mixed Bohm gyroBohm (mixed B/gB)

The mixed B/gB anomalous core transport model [14] can be expressed as follows:

$$\chi_e = 1.0\chi_{gB} + 2.0\chi_B \quad (1)$$

$$\chi_i = 0.5\chi_{gB} + 4.0\chi_B + \chi_{neo} \quad (2)$$

$$D_H = \left[0.3 + 0.7\rho\right]\frac{\chi_e\chi_i}{\chi_e + \chi_i} \quad (3)$$

$$D_Z = D_H \quad (4)$$

$$\chi_{gB} = 5\times10^{-6}\sqrt{T_e}\left|\frac{\nabla T_e}{B_\phi^2}\right| \quad (5)$$

$$\chi_B = 4\times10^{-5}R\left|\frac{\nabla(n_eT_e)}{n_eB_\phi}\right|q^2\left(\frac{T_{e,0.8} - T_{e,1.0}}{T_{e,1.0}}\right) \quad (6)$$

where, the χ_e is the electron diffusivity (m^2/s), χ_i is the ion diffusivity (m^2/s), D_H is the particle diffusivity (m^2/s), D_z is the impurity diffusivity (m^2/s), χ_{gB} is the gyro-Bohm contribution, χ_B is the Bohm contribution, χ_{neo} is the neoclassical diffusivity (m^2/s). This coefficient is calculated by the NCLASS module [15]. ρ is a normalized minor radius. $T_{e,0.8}$ and $T_{e,1.0}$ are the local electron temperatures at the normalized minor radius 0.8 and 1.0, respectively (eV), B_ϕ is the toroidal magnetic field (T). R is the major radius (m). n_e is the local electron density ($\times10^{20}m^{-3}$). q is the safety factor.

2.2 The pedestal formation model[8]

This model is to develop and describe a self-formation of the pedestal and the details structure of the pedestal. The pedestal formation model can be written as follows:

$$f_{s_x} = \frac{1}{1 + C_x\left(\frac{\omega_{E\times B}}{\gamma_{ITG}}\right)^2}\times\frac{1}{\max(1,(s-0.5)^2)} \quad (7)$$

where the variables are as follows. C_x is the optimization coefficient for each transport channel. Subscript x stand for i, e, H, or Z; ion, electron, hydrogenic, and impurity, respectively (C_i =4.32×10^3, C_e =3.91×10^3, C_H =1.19×10^2, and C_z =1.22×10^2;), γ_{ITG} is an approximation of the linear ion temperature gradient (ITG) growth rate, estimated as v_{ti}/R where v_{ti} is the ion thermal velocity, R is the major radius of plasma, s is the magnetic shear, the $\omega_{E\times B}$ is the flow shearing rate that is calculated by using the following equation:

$$\omega_{ExB} = \left|\frac{RB_\theta^2}{B_\varphi}\frac{\partial\left(E_r/RB_\theta\right)}{\partial\psi}\right| \quad (8)$$

ψ is the poloidal flux ,and E_r can be calculated as follows:

$$E_r = \frac{1}{Zen_i}\frac{\partial p_i}{\partial r} - v_\theta B_\phi + v_\phi B_\theta \quad (9)$$

where $\partial p_i/\partial r$ is the pressure gradient, v_θ and v_ϕ are the poloidal and toroidal velocities, respectively, B_θ and B_ϕ are the poloidal and toroidal magnetic fields, respectively, n_i is the ion density, Z is the ion charge number, and e is the elementary charge. The calculation of the toroidal

velocity is given in section 2.3. Note that the poloidal velocity is estimated using the NCLASS module [15].

To predict a self-formation of the pedestal uses the suppression function for each transport channel as shown in Eq. (7), we suppressed the anomalous core transport in every channel, which is calculated from the mixed B/gB model. Thus, the suppression of the ion thermal diffusivity (χ_{i_s}), the suppression of the electron thermal diffusivity (χ_{e_s}), the suppression of the particle diffusivity (D_{H_s}), and the suppression of the impurity particle diffusivity (D_{Z_s}), are given by

$$\chi_{i_s} = \chi_i \times f_{s_{ion}} \quad (10)$$

$$\chi_{e_s} = \chi_e \times f_{s_{electron}} \quad (11)$$

$$D_{H_s} = D_H \times f_{s_{Hydrogenic}} \quad (12)$$

$$D_{Z_s} = D_Z \times f_{s_{impurity}} \quad (13)$$

2.3 Toroidal velocity model[10]

This model assumes that the toroidal velocity (v_ϕ) is directly proportional to the local ion temperature (T_i) as follows:

$$v_\phi = cT_i \quad (14)$$

where $c = 1.43\times10^4$ is the coefficient in the expression for toroidal velocity and is determined by calibrating the model for v_ϕ against experiment data points for optimized shear *H*-mode plasma.

3. Results and Discussions

In this work, the simulations are carried out for 10 DIII-D *H*-mode discharges using the BALDUR integrated predictive modeling code. These discharges are taken from the International Profile Database [16]. Table 1 summarizes the engineering parameters for each discharge. These parameters are used for the boundary and initial conditions for the BALDUR code and also for the boundary conditions for the core-edge simulations which are taken to be a fixed value at the separatrix assuming that the separatrix temperature is 10 eV and that the separatrix density is 1×10^{17} m^{-3} in all simulations. The simulation results show that the predicted plasma profiles are higher than the experimental profiles due to the overpredition of the top of pedestal. The example profiles of electron temperature (T_e), ion temperature (T_i), electron density (n_e), and ion density (n_i) of DIII-D discharge number 82205 are shown in Fig.1.

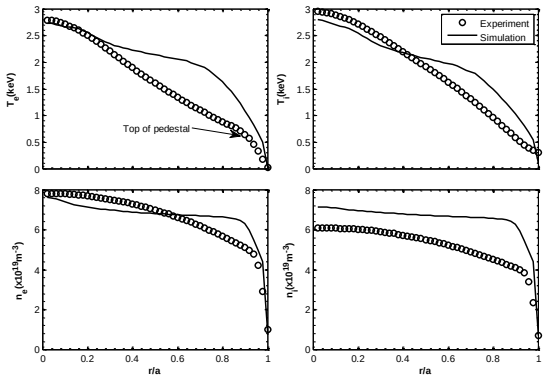

Fig.1. Profiles of electron temperature, ion temperature, electron density, and ion density as a function of normalized minor radius. The simulation results are carried out using BALDUR code. The results are compared to the DIII-D discharge 82205 at the diagnostic time**.**

In Fig.1, both the temperature and the density channels show high overprediction of the top of pedestal and profiles flat inside the plasma center to the plasma core (r/a: 0.0-0.4).This is due to the strong and the steep of E_r at the edge area as shown in Fig. 4. Moreover, the E_r shows the flat profile the deep core plasma to the center Thus, to quantify and to indicate the comparison between the simulation results and experimental results, we computed the root mean square (RMS) and offset(%). The RMS and offset are calculated as follows:

$$\mathrm{RMS}(\%) = \sqrt{\frac{1}{N}\sum_{i=1}^{N}\left(\frac{X_{\mathrm{sim}_i} - X_{\mathrm{exp}_i}}{X_{\mathrm{exp}_0}}\right)^2} \times 100 \quad (15)$$

$$\mathrm{offset}(\%) = \frac{1}{N}\sum_{i=1}^{N}\left(\frac{X_{\mathrm{sim}_i} - X_{\mathrm{exp}_i}}{X_{\mathrm{exp}_0}}\right) \times 100 \quad (16)$$

Table 1. Summary of engineering parameters for 10 DIII-D *H*-mode discharges at the diagnostic time. The parameters were used as boundary and initial conditions for BALDUR code.

Parameters	Discharges									
	77557	**77559**	**81321**	**81329**	**81499**	**81507**	**82205**	**82788**	**82188**	**82183**
Major radius, R (m)	1.68	1.69	1.69	1.70	1.69	1.61	1.69	1.68	1.69	1.69
Minor radius, a (m)	0.62	0.62	0.60	0.59	0.63	0.54	0.63	0.62	0.63	0.54
Elongation, κ	1.85	1.84	1.83	1.83	1.68	1.95	1.71	1.67	1.65	1.91
Triangularity, δ	0.33	0.35	0.29	0.36	0.32	0.29	0.37	0.35	0.29	0.22
Toroidal Magnetic Field, B_ϕ(T)	1.99	1.99	1.98	1.94	1.91	1.91	1.87	0.94	1.57	1.57
Plasma Current, I_p (MA)	1.00	1.00	1.00	1.00	1.35	1.34	1.34	0.66	1.33	1.33
Electron line average density, $\bar{n}_e(10^{19}\mathrm{m}^{-3})$	4.88	5.02	2.94	5.35	4.81	4.90	5.34	2.86	6.47	6.87
Effective Charge, Z_{eff}	1.68	2.21	2.42	1.65	2.33	1.93	2.13	1.94	1.95	1.95
Neutral Beam Power, P_{NB} (MW)	4.78	13.23	3.49	8.34	5.74	5.71	5.68	3.25	3.92	3.92
Diagnostic Time(s)	2.70	2.70	3.90	3.80	4.00	3.80	3.66	3.54	3.78	3.78

where X_{exp_i} is the i^{th} data point of the experiment profile, X_{sim_i} is the corresponding data point of the simulation profile, and X_{exp_0} is the maximum data point of the experiment profile of X as a function of the radius, which has N total number of data points. It should be noted that when the offset is positive, it indicates that the simulated profile is systematically higher than the experimental profile while a negative offset indicates that the simulated profile is systematically lower than the experimental profile. In Fig. 2, the RMS(%) of the electron temperature ranges from 30.78% to 13.52% in which the average value is 20.49%. In the case of ion temperature, the RMS(%) ranges from 20.11% to 9.27% and the average RMS(%) is 15.80%. In the case of electron density, the RMS(%) ranges from 15.29% to 7.11% and the average value of RMS(%) is 10.74%; moreover, the RMS(%) value of ion density ranges from 28.11% to 10.71%, and the average RMS(%) is 17.53%. Also, in Fig. 3, the offset(%) of four parameters are mostly positive, indicating that simulation overpredicts the experimental data. Especially, the temperature channels (T_e and T_i) are mostly value of offset(%), so strong suppression occurred due to strong optimization coefficients (C_e and C_i).

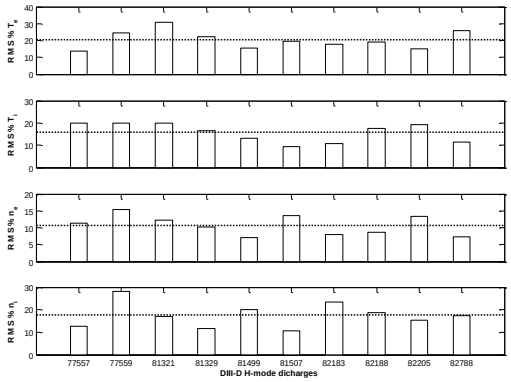

Fig.2. The RMS(%) for electron temperature, ion temperature, electron density, and ion density produced by a simulation using BALDUR code as compared to experimental data for 10 *H*-mode discharges by DIII-D device. The average of RMS(%) in each profile is shown by a dash line in each graph.

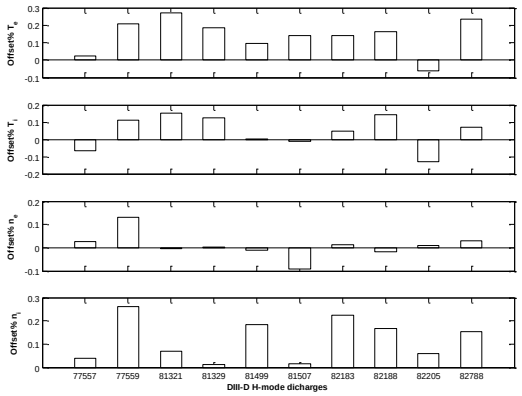

Fig.3. The offset(%) for electron temperature, ion temperature, electron density, and ion density produced by a simulation using BALDUR code as compared to experimental data for 10 *H*-mode discharges by DIII-D device.

For this study, the RMS(%) values and the offset(%) values in every parameter are mostly positive and are higher when compared to the previous work in Ref.[8]. Since the E_r as shown in Eq. (9) is calculated from three terms, the $\omega_{E\times B}$ flow shear is stronger than in the previous work as shown in Fig. 4. Moreover, the coefficients from a previous work set of the optimization coefficients for each transport channel was taken into account to perform these simulations. Thus, these coefficients in this work must be calibrated again. It should be noted that the BALDUR code is suitable for their simulations as mention in Section 2 about 10% RMS deviation when the simulations were carried out by using boundary conditions at the top of pedestal, however; when it is implemented the new model or the new calculation. The re-calibration must be performed for this work.

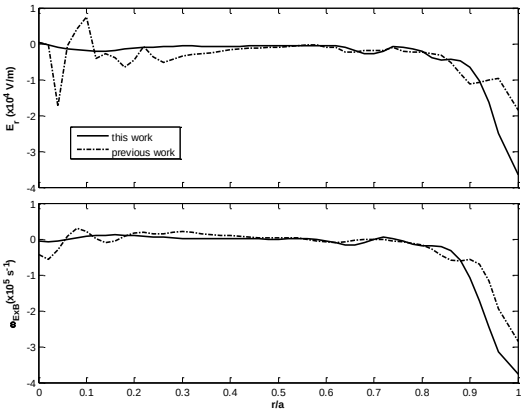

Fig.4. Simulation profiles of the radial electric field (top) and the $\omega_{E\times B}$ flow shear (bottom) as a function of a normalized minor radius. These simulation profiles compare two parameters between the calculation from this work and that from the previous work. They are taken from DIII-D *H*-mode experiments discharge 82205.

4. Conclusion

The simulation results, which are carried out through a full calculation of the radial electric field and the suppression model with all coefficients in each channel

show an overprediction in the core and especially in the edge region. The simulation results were higher than the experimental results of 10 DIII-D *H*-mode discharges as can be seen from the RMS% and offset% values because a strong $\omega_{E\times B}$ flow shear occurred at the edge area. Therefore, all coefficients used in this work came from the previous work that was calibrated the radial electric field from two quantities: pressure gradient and poloidal velocity.

5. References

[1] Connor, J. W. and Wilson, H. R., A review of theories of the L-H transition, Plasma Phys. Control. Fusion, Vol. 42, No. 1, pp. R1-R74, 2000.

[2] Aymar, R., Barabaschi, P., and Shimonura, Y., The ITER design, Plasma Phys. Control. Fusion, Vol. 44, No. 5, pp. 519, 2002.

[3] Hubbard, A. E., Physics and scaling of the *H*-mode pedestal, Plasma Phys. Control. Fusion, Vol. 42, No. 5A, pp. A15, 2000.

[4] Biglari, H., Diamond, P. H., and Terry, P. W., Influence of sheared poloidal rotation on edge turbulence, Phys. Fluids B-Plasma, Vol. 2, No. 1, pp. 1-4, 1990.

[5] Gohil, P., Edge transport barriers in magnetic fusion plasmas, Comptes Rendus Physique, Vol. 7, No. 6, pp. 606-621, 2006.

[6] Boedo, J., Gray, D., Jachmich, S., Conn, R., and Terry, G. P., Enhanced particle confinement and turbulence reduction due to ExB shear in the TEXOTR tokamak, Nucl. Fusion, Vol. 40, No. 7, pp. 1397, 2000.

[7] Oost, G. V., Adámek, J., Antoni, V., Balan, P., Boedo, J. A., Devynck, P., *et al.*, Turbulent transport reduction by E × B velocity shear during edge plasma biasing: recent experimental results, Plasma Phys. Control. Fusion, Vol. 45, No. 5, pp. 621, 2003.

[8] Pianroj, Y., Techakunchaiyanunt, J., and Onjun, T., Model for Pedestal Transport Based on Suppression of Anomalous Transport Using w_{ExB} Flow Shear and Magnetic Shear, J. Phys. Soc. JPN., Vol. 81, No. 044502, pp. 1-13, 2012.

[9] Pianroj, Y. and Onjun, T., Simulations of H-mode Plasma in Tokamak Using a Complete Core-Edge Modeling in the BALDUR Code, Plasma Sci. Technol., Vol. 14, No. 9, pp. 778-788, 2012.

[10] Chatthong, B., Onjun, T., and Singhsomroje, W., Model for toroidal velocity in H-mode plasmas in the presence of internal transport barriers, Nucl. Fusion, Vol. 50, No. 6, pp. 064009, 2010.

[11] Singer, C. E., Post, D. E., Mikkelsen, D. R., Redi, M. H., McKenney, A., Silverman, A., *et al.*, Baldur: A one-dimensional plasma transport code, Computer Physics Communications, Vol. 49, No. 2, pp. 275-398, 1988.

[12] Onjun, T., Bateman, G., and Kritz, A. H., Comparision of low confinement mode transport simulation using mixed Bohm/gyro-Bohm and the Multi-Mode 95 transport model, Phys. Plasma, Vol. 8, No. 3, pp. 975, 2001.

[13] Hannum, D., Bateman, G., Kinsey, J., Kritz, A. H., Onjun, T., and Pankin, A., Comparison of high-mode predictive simulations using Mixed Bohm/gyro-Bohm and Multi-Mode (MMM95) transport models, Phys. Plasma, Vol. 8, No. 3, pp. 964-974, 2001.

[14] Tala, T., Parail, V. V., and Becoulet, A., Comparison of theory-based and semi-empirical transport modeling in JET plasmas

with ITBs Plasma Phys. Control. Fusion, Vol. 44, No. 5A, pp. A495, 2002.

[15] Houlberg, W. A., Shaing, K. C., Hirshman, S. P., and Zarnstorff, M. C., Bootstrap current and neoclassical transport in tokamaks of arbitrary collisionality and aspect ratio, Phys. Plasma, Vol. 4, No. 9, pp. 3230, 1997.

[16] Boucher, D., Connor, J. W., Houllberg, W. A., Turner, M. F., Bracco, G., and et al., The International Multi-Tokamak Profile Database, Nucl. Fusion, Vol. 40, No. 12, pp. 1955, 2000.